Energy-Momentum Coupling in Radiating Shock Layers about a Blunt Body

Y. S. Chou* and L. H. Blake†
Lockheed Palo Alto Research Laboratory, Palo Alto, Calif.

This theoretical study investigated the flow in the thin shock layer about axisymmetric blunt bodies by a Blasius type series expansion technique. Solutions were obtained for three terms in the series, and the validity of the resulting solutions was shown to converge numerically away from the stagnation point to a body angle near the sonic line (~45°). The primary objective of the investigation was to determine the coupling experienced between the radiative and viscous transport. Consequently, solutions were obtained for both the viscous and inviscid models at three extreme Earth entry flight conditions. A real gas air model was considered. The radiation emission and absorption properties were described by a three-band continuum radiation model, and the differential approximation method was used to describe the radiative transport. A cold, nonblowing wall was assumed and the Prandtl number as well as the viscosity-density ratio were assumed constant. The results indicate a weak coupling between viscosity and the radiative flux distribution. The influence of radiative transport upon the convective heating is shown to be significant; however, the effect of radiative transport upon the velocity field is small.

Nomenclature

$A_{i,1}, A_{i,2} \ldots$ = coefficients in the series expansion for integrated intensity
B = blackbody radiation
B_ν = Planck function
c = speed of light
$f_1, f_2 \ldots$ = coefficients in the series expansion for tangential velocity
$g_1, g_2 \ldots$ = coefficients in the series expansion for total enthalpy
H = total enthalpy
h = specific enthalpy, Planck constant
I_ν = spectral radiation intensity
I_o = spatially integrated intensity
$\tilde{k}$ = $1 + ky$
k = body curvature, Boltzman constant
m = mass
N = mass density viscosity ratio $\rho_s\mu_s/\rho\mu$
N_N = number density of nitrogen atoms
p = pressure
Pr = Prandtl number
q^R = radiative heat transfer
q^C = convective heat transfer
$(q_x)_\nu, (q_y)_\nu$ = spectral radiative heat flux in the direction of x and y, respectively
r = distance measured from axis of symmetry
R_b = body radius of curvature at stagnation point
R_s = shock radius of curvature at stagnation point
Re = Reynolds number $\rho_\infty U_\infty R_s/\mu_{s(o)}$
T = temperature
u = velocity component parallel to the body
v = velocity component perpendicular to the body
x = distance parallel to the body measured from stagnation line
y = distance normal to the body
α_ν = absorption coefficient
β = degree of dissociation
γ = specific heat ratio C_p/C_v
Δ = shock layer thickness
ϵ = stagnation point density ratio across shock
η = normalized stream function
θ_d = dissociation energy
θ_i = ionization energy
ν = frequency
ξ_N = quantum mechanical correction factor for absorption coefficient
ρ = density
μ = viscosity
Ψ = stream function
λ_i = normalized optical depth associated with band i $\lambda_1 = 9\tilde{a}\rho_\infty R_s/m[kT_{s(o)}]^3$ $\lambda_2 = \lambda_3 = 5.16 \times 10^{-17}\rho_\infty R_s/m$
Γ = ratio of radiation energy to convective energy $2[kT_{s(o)}]^4/h^3c^2\rho_\infty U_\infty{}^3$
Γ_i = the value of Γ associated with band i, $\Gamma_1 = \lambda_1\Gamma$, $\Gamma_2 = \Gamma_3$, $\Gamma_2/\Gamma_1 = \lambda_2/\lambda_1$
δ = radiation cooling parameter, defined in Table 1

Subscripts

s = quantities at shock
b = quantities at body
(o) = quantities at stagnation line
N = nitrogen
∞ = freestream conditions

Received September 15, 1969; revision received January 29, 1970. This work was supported by NASA under Contract NAS 7-632. The authors would like to express their appreciations to K. H. Wilson for his helpful discussions and suggestions. Thanks are also extended to H. R. Kirch for her able IBM programming and suggestions on the numerical calculations.

* Associate Research Scientist. Member AIAA.
† Associate Research Scientist.

Introduction

In this study, the thermal environment experienced by an object entering planetary atmospheres at superorbital velocities is investigated. The aerodynamic heating of blunt bodies has been considered at the stagnation point (e.g., Refs. 1–4) and around the body (e.g., Refs. 5–8) for a variety of transport models at particular flight conditions and body geometries. In contrast to these investigations, this study is a theoretical assessment of the influence of coupling between the viscous and energy transport mechanisms in the geometrically thin-radiating shock layer away from the stagnation point. The influence of these coupling mechanisms upon the calculated convective and/or radiative wall heat fluxes is evaluated. This coupling analysis determines the effect of the boundary layer on the radiative heating to the body, the effect of the radiative transport on the velocity field, and the coupling between the radiative loss

and the convective heating. Results are presented at the stagnation point and around the body to the sonic line ($\sim 45°$).

The radiating flow was described by a Blasius series formulation for both inviscid and viscous models; solutions were obtained for three terms in the series. For the flight conditions considered, the three-term series solutions were shown to converge numerically for body angles approaching the sonic line ($\sim 45°$). A similar series representation has been shown to be adequate in describing the inviscid, adiabatic, hypersonic shock layer about a blunt body to the sonic line.[9] Transport models were used which retained the basic interaction influences but allowed for a simplified analysis. A real gas (air) model[10] was considered around a cold, nonablating spherical body. The radiative transfer was described by the well-known differential approximation. A three-band continuum radiation model was assumed where analytical expressions are available for the absorption coefficient in each band.[11] Solutions were obtained for both viscous and inviscid models at three sets of flight conditions which included extremes of the viscous and transport parameters.

Governing Equations

The fluid conservation equations (mass, momentum, energy) for axisymmetric bodies, written in a body oriented, coordinate system, are

$$\partial \rho u r/\partial x + \partial \rho v r \tilde{k}/\partial y = 0 \tag{1}$$

$$\rho u \frac{\partial u}{\partial x} + \rho v \tilde{k} \frac{\partial u}{\partial y} = -\frac{\partial p}{\partial x} + \frac{\partial}{\partial y}\left(\mu \frac{\partial u}{\partial y}\right) - \rho k u v \tag{2}$$

$$\tilde{k}(\partial p/\partial y) = k u^2 \rho \tag{3}$$

$$\rho u \frac{\partial H}{\partial x} + \tilde{k}\rho v \frac{\partial H}{\partial y} = \frac{\partial}{\partial y}\left(\frac{\mu}{Pr}\frac{\partial H}{\partial y}\right) + \frac{\partial}{\partial y}\left[\frac{\mu(1-1/Pr)}{2}\frac{\partial u^2}{\partial y}\right] + \int_0^\infty \alpha_\nu \left[\int_0^{4\pi} I_\nu d\Omega - 4\pi B_\nu\right] d\nu \tag{4}$$

The y momentum equation has been simplified by retaining only the terms of order unity.

The radiation field is coupled with the fluid mechanics through the integral term in the energy equation which represents the radiative energy loss or gain per unit volume.

In seeking solutions of the radiative transfer equation, we will use the differential approximation. In the present case of a geometrically thin hot gas with a cold wall and cool gas in front of the shock, the differential approximation has been suggested as a valid description of the radiative transport.[12]

In the framework of the differential approximation, the radiative transfer equation is approximated by the following set of equations:

$$\nabla \cdot q_\nu = -\alpha_\nu[(I_o)_\nu - 4\pi B_\nu] \tag{5a}$$

$$\partial (I_o)_\nu/\partial y = -3\alpha_\nu (q_y)_\nu \tag{6}$$

$$\partial (I_o)_\nu/\partial x = -3\alpha_\nu (q_x)_\nu \tag{7}$$

In the case of the thin shock layer, $\partial/\partial x \ll \partial/\partial y$, and we make the approximation that‡ $\nabla \cdot q_\nu \simeq \partial (q_y)_\nu/\partial y$.

Thus, Eq. (5a) becomes

$$\partial (q_y)_\nu/\partial y = -\alpha_\nu[(I_o)_\nu - 4\pi B_\nu] \tag{5b}$$

One immediate consequence of this thin layer simplification is that Eqs. (5b) and (6) are sufficient for the determination of q_y and I_o; Eq. (7) is only needed for calculating q_x.

‡ The error introduced by this approximation is shown to be of the order ϵ^2 (Ref. 13).

We will now consider only the absorption coefficient α_ν for continuum radiation and neglect the line and molecular band radiation. We will also take the three-band model for α_ν; namely, we approximate α_ν by three analytic expressions in three different frequency ranges of the spectrum. The specific form of α_ν and the range of frequency interval will be presented in the next section. Here we will represent the frequency interval generally by $(\Delta h\nu)_i$, $i = 1,2,3$. We then define

$$(\alpha q_y)_i = \int_{(\Delta h\nu)_i} \alpha_\nu (q_y)_\nu d\nu, \; (\alpha I_o)_i = \int_{(\Delta h\nu)_i} \alpha_\nu (I_o)_\nu d\nu, \; B_i = \int_{(\Delta h\nu)_i} \alpha_\nu B_\nu d\nu \tag{8}$$

Clearly

$$\alpha q_y = \Sigma_i (\alpha q_y)_i; \quad \alpha I_o = \Sigma_i (\alpha I_o)_i; \quad B = \Sigma_i B_i \tag{9}$$

With substitution of Eqs. (9), Eq. (4) and the radiative transfer Eqs. (5b) and (6) (after integration with respect to frequency) then become

$$\rho u \frac{\partial H}{\partial x} + \tilde{k}\rho v \frac{\partial H}{\partial y} = \frac{\partial}{\partial y}\left(\frac{\mu}{Pr}\frac{\partial H}{\partial y}\right) + \frac{\partial}{\partial y}\left[\mu\left(1-\frac{1}{Pr}\right)\frac{\partial}{\partial y}\left(\frac{u^2}{2}\right)\right] + \sum_{i=1}^{3}[(\alpha I_o)_i - 4\pi B_i] \tag{10}$$

$$\partial (q_y)_i/\partial y = -[(\alpha I_o)_i - 4\pi B_i] \tag{11}$$

$$\partial (I_o)_i/\partial y = -3(\alpha q_y)_i \tag{12}$$

We now proceed to normalize the variables. The distances x,y and the distance from the axis, r, are normalized by the stagnation point shock radius R_s, the velocities u,v by the freestream velocity u_∞, the density ρ by the freestream density ρ_∞, the pressure p by twice the freestream kinetic pressure $\rho_\infty u_\infty{}^2$, the body curvature k by $1/R_s$, the total enthalpy H as well as the static enthalpy h by H_s and, finally, the stream function ψ by $\rho_\infty u_\infty R_s{}^2$. The temperature is normalized by the temperature immediately behind the normal shock $T_{s(o)}$, the viscosity by its value immediately behind the normal shock $\mu_{s(o)}$ and q, I_o, B are all normalized by the quantity $[kT_{s(o)}]^4/h^3c^2$. From here on, the equations are all written in nondimensional form. The following transformation is now made:

$$\xi(x) = \epsilon \int_0^x \rho_s \mu_s dx, \; \eta(x,y) = \frac{\psi}{r_s{}^2}, \; d\psi = \rho u r dy - \rho v r \tilde{k} dx \tag{13}$$

We note for inviscid case $\xi = x$.

The conservation equations can then be written in ξ, η coordinates as

$$\rho u\left(r_s{}^2\frac{\partial u}{\partial \xi} - \eta \frac{dr_s{}^2}{d\xi}\frac{\partial u}{\partial \eta}\right) = -\left(r_s{}^2\frac{\partial p}{\partial \xi} - \eta\frac{dr_s{}^2}{d\xi}\frac{\partial p}{\partial \eta}\right) + \frac{N}{\epsilon Re}\rho u \frac{\partial}{\partial \eta}\left(u\frac{\partial u}{\partial \eta}\right) \tag{14}$$

$$\partial p/\partial \eta = k u r_s \tag{15}$$

$$\epsilon \rho_s \mu_s u\left[r_s{}^2\frac{\partial H}{\partial \xi} - \eta\frac{dr_s{}^2}{d\xi}\frac{\partial H}{\partial \eta} - \frac{N}{\epsilon Re Pr}\left(u\frac{\partial H}{\partial \eta}\right) - \frac{N}{\epsilon Re}\left(1-\frac{1}{Pr}\right)\frac{\partial}{\partial \eta}\left(u^2\frac{\partial u}{\partial \eta}\right)\right] = r_s{}^2 \Sigma_i \Gamma_i [(\alpha I_o)_i - 4\pi B_i] \tag{16}$$

$$u[\partial (q_\eta)_i/\partial \eta] = -\lambda_i r_s [(\alpha I_o)_i - 4\pi B_i] \tag{17}$$

$$u[\partial (I_o)_i/\partial \eta] = -3\lambda_i r_s (\alpha q_\eta)_i \tag{18}$$

with $i = 1,2,3$ and $Re = \rho_\infty U_\infty R_s/\mu_{s(o)}$.

In Eqs. (14) and (16) the following approximation and assumption were made; namely, $r \simeq r_s$ and $\rho\mu/\rho_s\mu_s = N = \text{const}$.

The boundary conditions for the flowfield are given as follows: at the shock, $\eta = \frac{1}{2}$, $u = u_s$, $p = p_s$, $\rho = \rho_s$, $H = H_s$,

Table 1 Properties for cases investigated

	Cases I	II	III
Freestream velocity, km/sec	16.0	18.0	11.0
Freestream density, $\rho_\infty(\times 10^{-7}$ g/cm$^3)$	4.21	1.0	10.0
Stagnation point shock radius, R_s (meter)	2.34	0.5	3.00
Normal shock density ratio, ϵ	0.057	0.055	0.065
Reynolds number, Re $[\rho_\infty U_\infty R_s/\mu_s(o)]$	216,000	18,000	128,000
Viscous parameter, $(\rho_w\mu_w/\rho_s\mu_s\epsilon Re)$	1.56×10^{-3}	3.04×10^{-2}	3.24×10^{-4}
Radiation cooling parameter, $\delta(2q_b/\frac{1}{2}\rho_\infty U_\infty^3)$	0.454	0.226	0.015

and H_s, u_s, p_s, ρ_s are given by oblique shock relations; at the body, $\eta = o$, $u = o$, $H = g_b$.

For the radiation field, the differential approximation gives us the condition: at the shock, for cold gas ahead of the shock, we have $I_o - 2q_y = 0$, which then implies $(I_o)_i - 2(q_y)_i = 0$ for all i. At the body, the cold wall assumption $I_0 + 2q_y = 0$. Thus, $(I_o)_i + 2(q_y)_i = 0$, for all i.

Gas Properties

Curve fitting of the equilibrium properties of air calculated in Ref. 10 suggests the following approximate equation of state: $p = 10^{-2.5}\rho(h/R)^{0.84}$ with p in atm, ρ is amagat, and h/R in °K. This then implies that in the normalized form, the equation of state is

$$p/p_s = (\rho/\rho_s)(h/h_s)^{0.84} \tag{19}$$

Another equation of state for air is also available, namely

$$\rho = 1.65 \times 10^{-5} p(T/10^4)^{-1.72} \text{g/cm}^2 \tag{20}$$

where p is in atm and T is in °K. Equations (19) and (20) thus completely specify the equilibrium thermodynamic properties in air.

In the calculation of absorption coefficients, the contributions from ions are neglected and we treat oxygen as if it were nitrogen; therefore, we model air by pure nitrogen gas. The analytical expressions for the absorption coefficients are taken from Hoshizaki and Wilson.[5] They are written as

$$\alpha_\nu = (1 - e^{-h\nu/kT})(K_\nu)_N \tag{21}$$

with

$$(K_\nu)_N = 4.5\tilde{a}N_N kT e^{-(14.3-h\nu)/kT}\ \xi_N/(h\nu)^3;\quad 0 \le h\nu \le 4.22$$

$$(K_\nu)_N = 4.5\tilde{a}N_N kT[\xi_N/(h\nu)^3]e^{-10.08/kT};\quad 4.22 \le h\nu \le 10.8$$

$$(K_\nu)_N = N_N \cdot \varphi_{N,1};\quad 10.8 < h\nu \le 12.0$$

$$(K_\nu)_N = N_N(\varphi_{N,1} + \varphi_{N,2});\quad 12.0 < h\nu \le \infty$$

and

$$\varphi_{N,1} = 5.16 \times 10^{-17} e^{-3.5/kT}/(4 + 10e^{-2.38/kT} + 6e^{-3.57/kT})$$

$$\varphi_{N,2} = 6.4 \times 10^{-17} e^{-2.3/kT}/(4 + 10e^{-2.38/kT} + 6e^{-3.57/kT})$$

$$\tilde{a} = 7.28 \times 10^{-16}\text{cm}^2 - \text{ev}^2$$

where N_N is the number density of nitrogen atoms and ξ_N is the quantum mechanical correction factor. We approximate ξ_N by

$$\xi_N = 0.24 + 0.426(h\nu - 4.22)^2 \tag{22}$$

The ranges of the three-band model are chosen as $(\Delta h\nu)_1$, $0 \le h\nu \le 10.8$, $(\Delta h\nu)_2$, $10.8 \le h\nu \le 12$, $(\Delta h\nu)_3$, $12 \le h\nu \le \infty$ when the unit of $h\nu$ is in ev.

In the first band $(\Delta h\nu)_1$, α_ν is small, and the optical depth (in this range of frequency and based on the shock layer thickness) is much less than unity. Hence it is reasonable to approximate α_ν in this range by its partial Planck mean, defined as [denoting dimensional quantities by (′)]

$$\alpha_1' = \int_{(\Delta h\nu)_1} \alpha_\nu B_\nu d\nu / \int_{(\Delta h\nu)_1} B_\nu d\nu$$

In the second and third bands, $h\nu/kT$ is large, consequently $e^{-h\nu/kT} \ll 1$. We therefore can take α_2', α_3' as independent of frequency, i.e., $\alpha_2' = N_N\varphi_{N,1}$, $\alpha_3' = N_N(\varphi_{N,1} + \varphi_{N,2})$. Based on these considerations, one finds $(\alpha' q_y')_i = \alpha_i'(q_y')_i$, $(\alpha' I_o)_i = \alpha_i'(I_o)_i$.

The atom number density N_N is related to the total number density (and eventually density) by taking the following model. Namely, we assume that there will be no ionization before the gas is totally dissociated. In the dissociation phase, we relate the atom number density to the total number density by using the Lighthill's ideal dissociation model. For the ionization phase, we assume the gas is in Saha equilibrium.

Methods of Solution

The shock conditions are described by their Taylor Series expansion away from the stagnation point.[13] From the form of the shock condition series, the dependent variables of Eqs. (14–18) are written as a power series of ξ with coefficients that are a function of η. The solutions can thus be written

$$u = f_1(\eta)\xi + u_1 f_2(\eta)\xi^3 + u_2 f_3(\eta)\xi^5 + \ldots \tag{23a}$$

$$H = g_1(\eta) + g_2(\eta)\xi^2 + g_3(\eta)\xi^4 + \ldots \tag{23b}$$

$$(I_o)_i = A_{i,1}(\eta) + A_{i,2}(\eta)\xi^2 + A_{i,3}(\eta)\xi^4 + \ldots \tag{23c}$$

$$(q_y)_i = Q_{i,1}(\eta) + Q_{i,2}(\eta)\xi^2 + Q_{i,3}(\eta)\xi^4 + \ldots \tag{23d}$$

where u_1, u_2, u_3 are constants governed by the shock shape. From the series expansions of the shock conditions and Eqs. (23), the radiation and thermodynamic variables can be written in series form. Substituting the resulting series expansion of the dependent variables into the governing Eqs. (14–18), and collecting like powers of ξ, the coefficients of Eqs. (23) are obtained from the resulting sets of equations.[13]

Solutions were obtained for the viscous case by the standard iterative numerical integration techniques of two-point boundary value problems. In the inviscid case, the indeterminacy problem as η approached zero was overcome by imposing the following conditions. Near the wall we demanded the velocity gradient to be bounded and the gas to be in radiative equilibrium so that the radiative flux divergence is zero.

The inputs of the freeflight conditions (velocity and density), stagnation point shock radius, Prandtl number, and the viscous parameter $N/\epsilon Re$ are necessary in the numerical calculations. In that the coordinate system used in the formulation was body oriented, an assumed shock shape is required. The shock shape is input through the constants of the parameter series expansion along the shock [Eq. (23a)]. These constants are, for a given body, all a function of the bluntness parameter B_s. (Assuming the shock is conical in shape.) The values of B_s can be found by first assuming a value, then adjusting it to fit the calculated shock shape. First guess values of B_s in this report were taken directly or extrapolated from the curve given in Lomax and Inouye.[14] No iteration on B_s is carried out in this study.

As one of the prime objectives of this investigation was to evaluate the influence of coupling between the momentum

and energy transport mechanisms, solutions were obtained for both viscous and inviscid flow. Flight conditions and body dimensions§ applicable to the hyperbolic entry problem[15] which produced the maximum coupling effects were used. Table 1 is a summary of the parametric conditions of the three cases investigated and Fig. 1 illustrates the corresponding regions of interest on a thermodynamic properties plot of entry conditions. The computational time on an 1108 computer per solution (three terms) ranged from $1\frac{1}{2}$ min. for an inviscid case to 4 min. for a viscous run.

Results

Validity of Series Solutions

The utility of the Blasius types series used in Eqs. (23) (like any series method) is restricted in that its global accuracy for a finite number of terms can only be evaluated by a comparison with an "exact" solution for a given problem. In this manner, Chou[9] showed that his closed form Blasius series solution (three-term series) of the adiabatic inviscid thin shock layer was most effective ($\pm 5\%$) in predicting the gasdynamics about a variety of bodies to the sonic line. For the viscous and inviscid radiating flow of a thin shock layer about a body, no "exact" solutions exist for comparison. The validity of a finite series solution to these radiating flow models may, therefore, only be assessed by indirect arguments.

The same form of series expansions were used in this investigation as was found successful in the adiabatic inviscid solutions of Chou.[9] As the radiative flux addition to the energy equation influences the gasdynamics only indirectly through the density field, it was anticipated that the radiation flux would affect the gasdynamics of the flow by a small effect. The coupling results discussed later in this section showed this to be true for both the inviscid and viscous models.

The validity of the series solution for each parameter must rest on two factors: 1) the numerical convergence of the series solution, and 2) the physical interpretation of the results. Consequently, the region of numerical convergence of the enthalpy series and the corresponding radiative energy flux are discussed.

Figure 2 illustrates the numerical convergence of the enthalpy profile at two different body angles. At 45°, the deviation from second to third term is approximately 20%. The results of applying Shanks nonlinear transformation[16] to the first three terms in the series are given. The Shanks transformation represents an approximate method of predicting the converged solution of a series expansion given three or more terms of the series. This transformation technique has been utilized by Van Dyke[17] as an indication

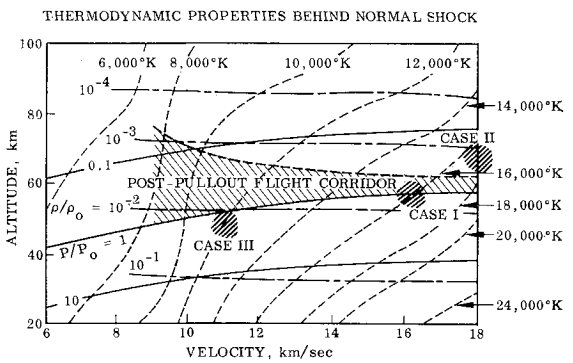

Fig. 1 Freestream conditions.

§ $11 \leq u_\infty \leq 18$ km/sec; $10^{-7} \leq \rho_\infty \leq 10^{-6}$ g/cm^3; $50 \leq R_s \leq 300$ cm.

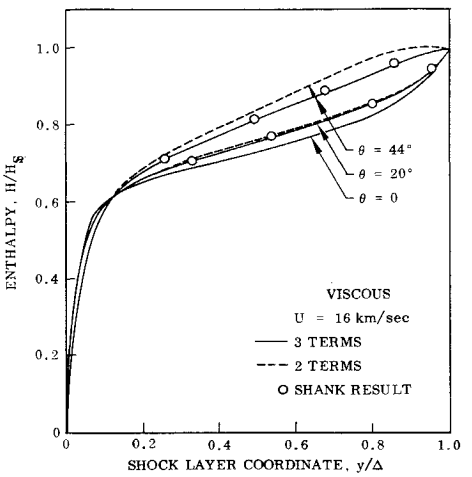

Fig. 2 Numerical convergence of enthalpy distribution ($\theta = 20°, 44°$).

of the rate of series convergence. A comparison of the Shanks results with the third-term solution indicates that a three-term expansion is effective in describing the enthalpy field to a body angle of 45°.

The numerical convergence of the radiative and convective energy fluxes to the wall is shown in Fig. 3. The results of the Shanks enthalpy distribution indicate the three-term series to be a valid solution to the sonic line (~45°). It should be noted here that the radiative flux was obtained from a solution of Eqs. (17) and (18) once the enthalpy distribution was calculated rather than from the series given by Eq. (23d). (For details, see Ref. 13.) Figures 2 and 3 are illustrative of the results of the three cases investigated. They show the three-term series solution numerically converges to the Shanks results ($\pm 5\%$) to a body angle near the sonic line (~45°).

The nature of the enthalpy and velocity distribution through the shock layer for different body angles is shown in Fig. 4. For the inviscid region the increase of the total enthalpy away from the stagnation point results from the

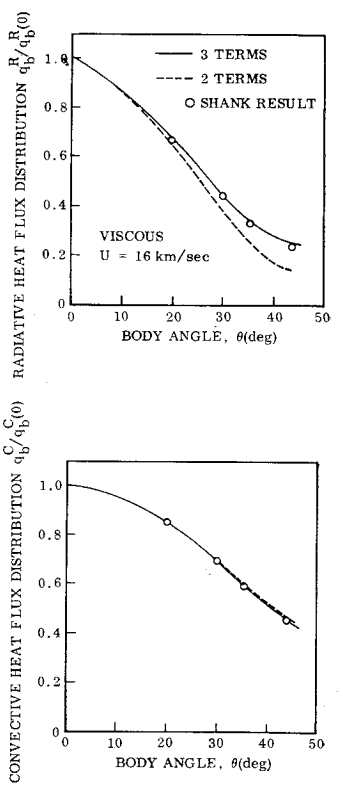

Fig. 3 Numerical convergence of radiation and convective heat fluxes.

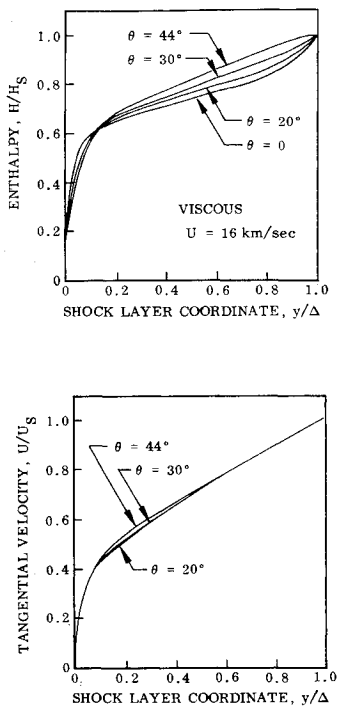

Fig. 4 Characteristic enthalpy and velocity distributions vs body angle.

expected increase in velocity and decrease in radiative heat loss of the flow as it leaves the stagnation region. The conductivity in the boundary layer increases the boundary-layer thickness and correspondingly decreases the convective heat flux.

The negligible variation of the velocity profiles about the body as shown in Fig. 4 were found to be very interesting. This insensitivity to body angle suggests the coupling from the enthalpy distribution to the momentum field is weak. This coupling will be discussed further in the results section.

Comparative Results

A comparison of the enthalpy, velocity and heat flux results for the three flight conditions¶ considered (Table 1) is presented in Figs. 5 and 6. The relative effects of the three flight conditions upon the resulting enthalpy and velocity profiles in the shock layer and the heat flux distribution at and away from the stagnation point will be considered.

Illustrative enthalpy and velocity results are shown in Fig. 5. The results presented are for a representative body angle of 36° for both the viscous and inviscid models. The magnitude of radiative and viscous transport govern the enthalpy and velocity distributions. Although radiative transport will thicken the boundary layer somewhat, the general boundary-layer distribution is a direct function of the magnitude of viscosity. Comparing the magnitudes of the viscous parameters in Table 1 for the three cases, the largest viscous influence is anticipated for the 18 km/sec case. This is substantiated by the enthalpy and velocity boundary-layer profiles noted in Fig. 5. The 16 and 11 km/sec cases have significantly less viscous influence as is demonstrated by their decreased boundary-layer thicknesses. Correspondingly, the viscous velocity profiles of the latter two cases differ only slightly from the inviscid runs near the wall.

The significant influence of the radiative transport is observed in the inviscid region of the enthalpy distributions. Having comparable cooling parameters, δ, the 16 and 18 km/sec cases experience similar enthalpy profiles in the inviscid region. In contrast, the small cooling parameter of the 11 km/sec case results in an enthalpy profile approaching that of an adiabatic flow.

The conformity of the velocity results in the inviscid region indicates the influence of the radiative transport upon the velocity field is small. This coupling will be discussed in detail in subsequent paragraphs of this section.

Figure 6 illustrates the relative comparison of the convective and radiative heat fluxes about the body. The differences in the distributions demonstrate the significance of the free-stream condition upon the convective and radiative heat loads about the body. The radiative flux is a direct function of the temperature level in the shock layer. At high temperatures, the radiative properties of emission and absorption are less sensitive to temperatures than at the lower temperature levels. Consequently, even though the temperature change in the shock layer away from the stagnation point is the greatest in the high-velocity case** (18 km/sec), the change of radiative heat flux about the body for this case is the least for the three considered. In the 11 km/sec case, the temperature change about the body is the least, however, the temperature level is sufficiently low that a small temperature change results in a significant influence upon the radiative properties. This is demonstrated by the correspondingly large radiative flux change for this case about the body as shown in Fig. 6.

The thickening of the enthalpy boundary layer away from the stagnation point accounts for the general decrease in convective heating. The relative convective heating distributions compare with the respective gradients of the enthalpy profiles of Fig. 5 at the wall. The 11 and 16 km/sec cases experience essentially the same convective heating while the large viscous influence of the 18 km/sec case produces a marked change from the other two. Because of the strong temperature dependence of the radiative flux, the change in radiative flux about the body is more pronounced for all cases than the corresponding changes in convective heating. Due to the high radiative heat flux experienced at the stagnation point of a blunt body, however, the radiative heating is far from negligible at the sonic line.

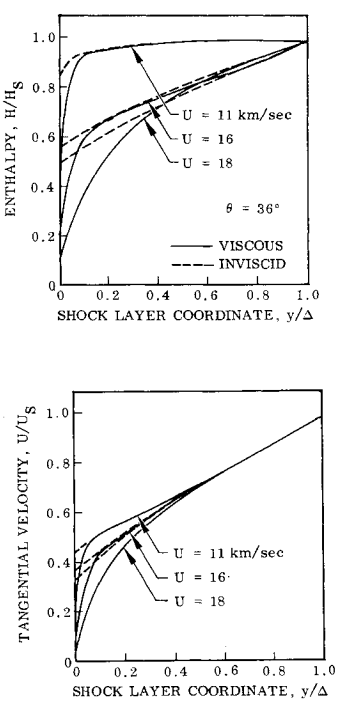

Fig. 5 Enthalpy and velocity distributions for three stream cases (θ = 36°).

¶ In this discussion, the freeflight velocities are used as the identification of the three cases considered.

** Because of the low velocity at the stagnation point, the stagnation point temperature is a direct function of the free-stream velocity.

Momentum and Energy Coupling

An understanding of the degree of coupling between the momentum and energy transport mechanisms was the prime objective of this investigation. Such an understanding could provide the justification for simplifying approximations in obtaining solutions of the radiating flow about a body. Such approximations would be essential should detailed treatment of the radiative and collisional transport be required.

The comparison of the radiative heat fluxes for both viscous and inviscid models away from the stagnation point for the three cases considered is presented in Fig. 7. The stagnation point radiative heat flux for each case is noted for comparison. As was expected, the inviscid model yielded the higher radiative cooling; however, the difference between the viscous and inviscid models was surprisingly small for all three cases. The influence of viscosity upon the radiation wall flux was only experienced beyond approximately 30°. Being a direct function of temperature, this difference in the radiative fluxes is attributed to the influence of viscosity on the thickening of the boundary layer. As the flow proceeds about the body, a greater portion of the total radiative heat flux comes from the boundary-layer region; therefore, the influence of the viscosity is experienced more dramatically far from the stagnation point. The resulting deviations are shown to be significant near the sonic line with the viscous results below the inviscid case as indicated in Fig. 7. Consequently, the primary effects of viscosity on the radiative heat fluxes is beyond a body angle of approximately 40°. In the stagnation region, the inviscid analysis yields an accurate description of the radiative heating for the range of Reynolds numbers and radiative coupling levels studied.

The effect of the radiation transport upon the convective heating load about a body is illustrated in Fig. 8. Because of the complexity added to the viscous energy equation by the divergence of the radiative flux, the error produced in the convective flux by its omission is of interest. The stagnation point convective heat flux results show the radiative transport can have an appreciable influence on the convective loss. As one would anticipate, the radiative heat loss thickens the boundary layer resulting in a lowering of the convective losses. Because of the large viscous effect in the 18 km/sec

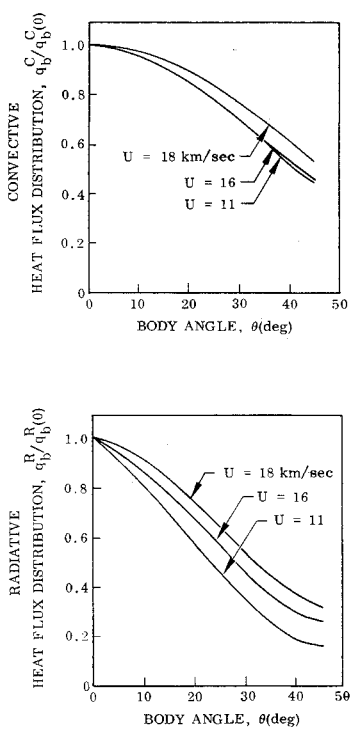

Fig. 6 Convective and radiative heat flux distributions for three freestream cases.

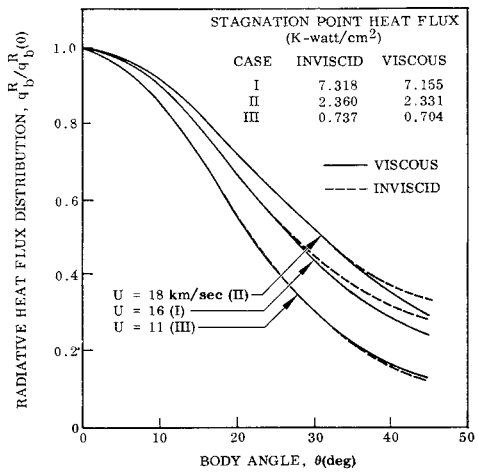

Fig. 7 Coupling of viscosity and radiative heat flux.

case, this influence is seen to effect this case less than the other two. (The 11 and 16 km/sec results were essentially the same.) Consequently, the results of Figs. 7 and 8 indicate the radiative heat flux determined by neglecting the flow viscosity can overpredict the radiative loss by less than 15%, but an overprediction of 35% in the convective heat flux can be experienced when the radiative transport is neglected in the energy equation.

Figure 9 illustrates the influence of the radiative transport upon the velocity field for both the viscous and inviscid flow models. As the heating load distributions are of prime importance, this coupling is shown indirectly by comparing the influence of two velocity fields upon the radiative heating flux, one from a completely coupled calculation and one from a nonradiating solution. It should be recalled that the momentum transport is only effected indirectly by the energy field through the density. The results shown in Fig. 9 indicate this coupling to be weak at the stagnation point. The "momentum without radiation" results are from the solution of the energy equation using a solution to the momentum equations obtained from a nonradiating flow calculation. For the inviscid model, this velocity field represents the adiabatic inviscid series solution of Chou.[9] For the viscous case, the velocity field was determined from a solution of the combined energy and momentum equations without the radiative flux divergence term.

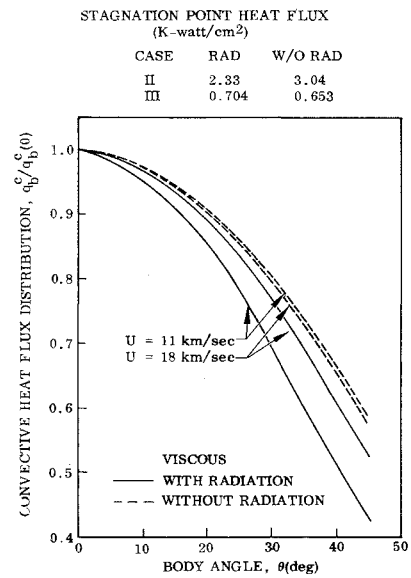

Fig. 8 Coupling of radiative transport to the convective heat flux.

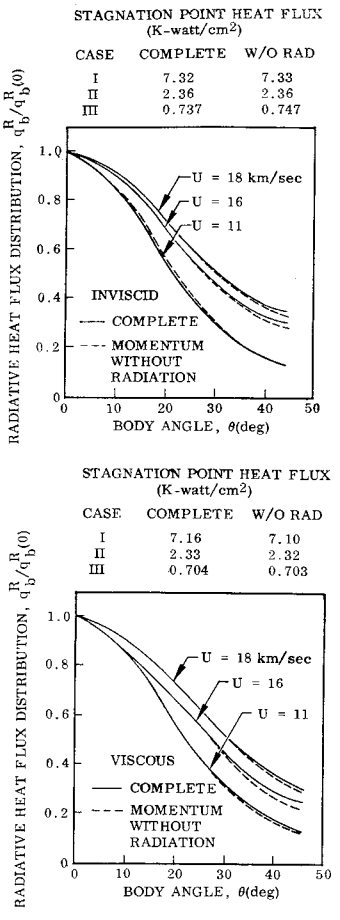

Fig. 9 Coupling of radiative transport to the velocity field.

The results of Fig. 9 indicate the weak coupling of the radiative transport on the velocity field as the latter influences the radiative flux away from the stagnation point. The results of Fig. 7 indicate that an accurate description of the radiative heat flux can be obtained by the solution of the energy equation using the adiabatic inviscid velocity distribution.

Conclusions

A three-term series formulation of the viscous and inviscid, radiating-absorbing flow in a geometrically thin shock layer about an axisymmetrical body has been completed. The radiative transport was modeled with a three-band continuum absorption coefficient and was described by the differential approximation. Solutions for each of the three terms in the series were obtained for a spherical body at three flight conditions which provide a wide variation in the effects of viscosity and radiative cooling. The three-term solutions were compared with the results of a Shanks nonlinear transformation of the series; numerical convergence was thus confirmed for the enthalpy and velocity series away from the stagnation point to a body angle near the sonic line. Having obtained an enthalpy distribution, the radiative heat flux was found from the solution of the radiative transport equation, since the radiative heat flux series was shown to slowly converge.

The radiative and convective heating distributions were obtained to a body angle of 45° for the three cases considered. The coupling between the momentum and energy transport was evaluated by comparisons of the convective and radiative flux distributions at and away from the stagnation point. This coupling analysis indicated that the influence of viscosity on the radiative heat flux calculation was small (<15%). The radiative transport was shown to effect the convective heat flux more strongly. The convective heating may be increased by 35% near the sonic line when the radiative transport is neglected. The influence of the radiative transport on the velocity field was shown to be small. The radiative flux results obtained by using a velocity field obtained from a nonradiating flow calculation was shown to agree very closely with the results of the fully coupled analysis.

These results suggest that an accurate description of the radiation heating about a blunt body can be obtained from an uncoupled solution of the energy equation with an adiabatic inviscid description of the velocity field.

References

[1] Biberman, L. M. and Bronin, S. Ya., "Theory of Heating in Hypersonic Flow," Soviet Physics-Doklady, Vol. 13, No. 9, 1969, p. 832.

[2] Anifimov, M. A. and Shari, V. I., "Solution of Motion Equations of a Selectivity Radiating Gas in a Shock Layer," *Izvestia An SSSR, Mekhanizm Khidk i Gaza*, No. 3, 1968, p. 18.

[3] Howe, J. R. and Viegas, J. R., "Solutions of the Ionized Radiating Shock Layer, Including Reabsorption and Foreign Species Effects, and Stagnation Region Heat Transfer," TR-R-159, 1963, NASA.

[4] Page, W. A. et al., "Radiation Transport in Inviscid Nonadiabatic Stagnation-Region Shock Layers," AIAA Paper 68-784, Los Angeles, Calif., June 1968.

[5] Hoshizaki, H. and Wilson, K. H., "Convective and Radiative Heat Transfer during Superorbital Entry," *AIAA Journal*, Vol. 5, No. 1, Jan. 1967, pp. 25–35.

[6] Cheng, P. and Vincenti, W. G., "Inviscid Radiating Flow Over a Blunt Body," *Journal of Fluid Mechanics*, Vol. 27, Pt. 4, 1967, pp. 625–646.

[7] Belotserkovski, O., "Supersonic Gas Flow around Blunt Bodies," Chap. V, 2nd ed., Computer Center of Academy of Sciences USSR, Moscow, 1967.

[8] Bogolepov, V. V. and Neiland, V. Ia., "Convective Heat Exchange in a Radiating Gas," *Mekhanizm Zhidk i Gaza*, No. 6, 1966, p. 23.

[9] Chou, Y. S., "Inviscid Hypersonic Flow Past Blunt Bodies," *AIAA Journal*, Vol. 7, No. 1, Jan. 1969, pp. 149–150.

[10] Neel, C. A. and Lewis, C. H., "Interpolation of Imperfect Air Thermodynamics Data," Rept. AEDC-TDR-64-184, Sept 1964, Arnold Engineering Development Center.

[11] Biberman, L. M. and Norman, G. E., "Recombination Radiation and Brehunstralung of a Plasma," *Journal of Quantitative Spectroscopy & Radiative Transfer*, Vol. 3, No. 3, 1963, pp. 221–245.

[12] Vincenti, W. G. and Kruger, C. H., Jr., *Introduction to Physical Gas-dynamics*, Chap. XII, Wiley, New York, 1965.

[13] Chou, Y. S. and Blake, L. H., "Thin Radiating Shock Layer About a Blunt Body," Rept. LMSC-687171, April 1969, Lockheed Missiles & Space Co.; also NASA CR-1547.

[14] Lomax, H. and Inouye, M., "Numerical Analysis of Flow Properties About Blunt Bodies Moving at Supersonic Speeds in an Equilibrium Gas," TR R-204, 1964, NASA.

[15] Syvertson, C. A., "Entry and Landing Requirements for Manned Planetary Missions," *AIAA Technology for Manned Planetary Missions Meeting*, AIAA, New York, 1968.

[16] Shanks, D., "Non-Linear Transformations of Divergent and Slowly Convergent Sequences," *Journal of Mathematics and Physics*, Vol. 34, 1955, pp. 1–42.

[17] Van Dyke, M., "Hypersonic Flow Behind a Paraboloidal Shock Wave," *Journal de Mécanique*, Vol. 4, No. 4, Dec. 1965, pp. 477–493.